

# Visualization and Animation of Inverter-Driven Induction Motor Operation

A. P. Sakis Meliopoulos, W. Gao  
Electrical and Computer Engineering  
Georgia Institute of Technology  
Atlanta, Georgia 30332  
Sakis.Meliopoulos@ece.gatech.edu

George J. Cokkinides  
Electrical and Computer Engineering  
University of South Carolina  
Columbia, SC 29208

**Abstract:** This paper discusses a new model of an inverter-driven induction motor that enables direct animation and visualization of the inverter and motor operation. The models of the inverter and induction motor are physically based model in actual quantities. As such they enable direct animation and visualization of the operation of the inverter-driven induction motor. The paper discusses the models and the animation and visualization approach. Specifically, the animation and visualization screens are discussed in terms of the displayed information. The implementation is in Open GL that permits rendering as well as rotation, panning, and zooming in real time. The paper presentation is by means of a live presentation of the animation and visualization models.

## Introduction

Inverter-driven induction motors have many advantages: (a) use of rugged and inexpensive induction motors without the disadvantage of high starting currents, and (b) speed control over a wide range, and (c) economic operation in applications of variable speed. Intensive research activities focus on improvements of inverter-driven induction motors. This research can be facilitated with high fidelity models of these systems and animation and visualization methods. This paper presents such an approach.

The paper first presents the computational engine, the model of the inverter-driven induction motor and the approach towards the animation and visualization. Specific examples are provided.

## The Virtual Power System Concept

Recent advances in software engineering have made it possible to develop dynamic system simulators that operate in a multitasking environment. The addition of graphical user interface tools and hardware-accelerated graphics make the final product an indispensable tool to the understanding of the operation of the system. Many products have been developed along these lines for power system engineering. Most of these are focused on simulating the system under sinusoidal steady state operation. Projecting the capabilities of the new technologies, claims of replacing physical laboratories with a virtual environment have surfaced. A virtual laboratory should have the following features:

1. Continuous simulation of the system under study.
2. Ability to modify the system under study during the simulation, and immediately observe the effects of the changes.
3. Provide advanced output data visualization options such as animated 2-D or 3-D displays that illustrate the operation of any device in the system under study.

The above properties are fundamental for a virtual environment. The first property guarantees the uninterrupted operation of the system under study in the same way as in a physical laboratory: once a system has been assembled, it will continue to operate. The second property guarantees the ability to connect and disconnect devices into the system without interrupting the simulation of the system. This property duplicates the capability of physical laboratories where one can connect a component to the physical system and observe the reaction immediately. For example connecting a motor to the power supply and observing the startup transients, etc. The third property duplicates the ability to observe the simulated system operation, in a similar way as in a physical laboratory.

In principle, the minimal requirements of a virtual environment can be achieved with present software and hardware technology. However, this task is nontrivial. For example, simulation methods that will accurately capture the system response under all possible conditions require wide band models for all power system components. This fact becomes apparent if one considers specific examples such as a power transformer. Nevertheless the technology exists to achieve all three requirements of a virtual environment. On the other hand, once a virtual environment has been developed, it can be of greater educational value than a physical laboratory. For example, in a physical laboratory we are limited as to what we can directly observe. Consider an electric motor. In a physical laboratory we can observe the motor speed, measure the torque etc., but we cannot observe the inner workings of the motor, magnetic field distribution and interaction, small rotor oscillations, etc. A virtual laboratory can provide this information using appropriate visualization techniques. In a physical laboratory, most fast transients will be missed because of limitations in human observability speed. A virtual laboratory can provide this capability. For, example, the operation of the system can be

slowed down or paused and restarted to study a specific fast transient condition.

In the past few years, we have undertaken an effort to explore the development of a virtual simulation environment. The central piece of this effort is a time domain simulator of dynamical systems in a multitasking environment. In this environment, visualization objects have access to the instantaneous conditions of the components and the overall system. Thus detailed 3-D “movies” of the instant-by-instant operation of the component or the system can be generated. This paper presents the application of this technology to inverter-driven induction motors.

The paper provides a brief overview of the new tool, the mathematical formulation of the simulator and the data flow between the time domain simulator and the visualization objects. The paper focuses on the inverter-driven induction motor. It presents the modeling of this system and the approach towards the animation and visualization of this system.

### Description of the Virtual Power System Environment

The internal structure of the Virtual Power System environment is illustrated in Figure 1. This architecture was developed with consideration on the minimal representation of system components and the requirements of a virtual environment. In the background is the network solver that is a time domain simulation program. The network solver is based on the representation of each system component with its *algebraic companion form (ACF)* [1]. The ACF is developed from the integro-differential equations of a component by numerical integration. The ACFs of all components in a system are related via the connectivity constraints. Application of the connectivity constraints yields a quadratic network equation that is solved at the network solver.

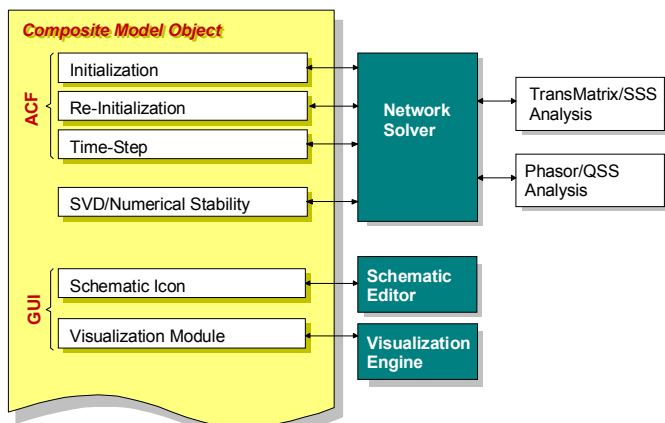


Figure 1. The Virtual Test Bed Architecture

The network solver is continuously executed providing the simultaneous solution of the entire system and determines the state of each component of the system. This information is passed back to the individual devices for animation and visualization of a specific component or groups of components. The Virtual Test Bed has been developed in a multitasking environment, thus allowing parameter changes and immediate system response observations.

Any power system component can be modeled in such a way that it can be interfaced with the Virtual Power System. Appendix A describes the procedure for an induction machine. The point is made that the model development of the induction machine is physically based, i.e. the stator as well as the rotor are explicitly represented in their own variables, in other words no convenient transformations are used. This is important for animation and visualization since the actual physical quantities can be displayed. In the case of the induction motor, one can observe the frequency of the rotor currents and how it changes as the induction machine accelerates or decelerates. The inverter model is also similarly modeled.

### Example System

This example illustrates the dynamics associated with an inverter-driven induction motor. The overall system is illustrated in Figure 2. It consists of a source, a transmission line, a transformer, a rectifier, an inverter and an induction machine and the mechanical load of the induction motor.

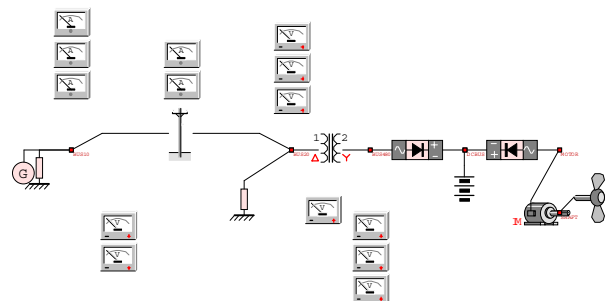
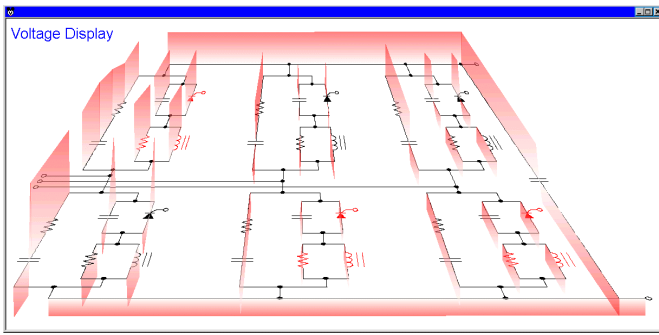
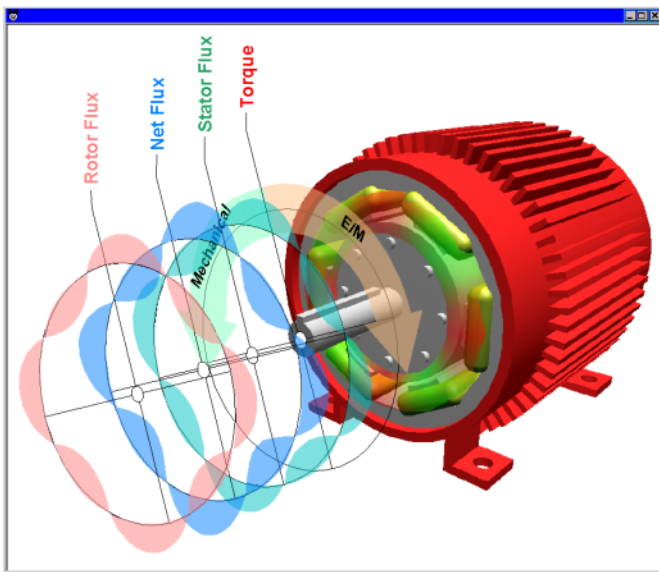


Figure 2. Example System of Inverter-Driven Induction Motor and Mechanical Load

The figure illustrates a number of meters that monitor various physical quantities of the system, i.e. speed, torque and voltage versus time plots. In addition to these graphs, two animation objects are included which show the operation of the inverter and the operation of the induction motor in an animated way. A snapshot of the animation is shown in Figures 3 and 4.



**Figure 3. A Snapshot of the Animation of the Inverter Showing the Voltage Distribution Along the Circuits of the Inverter.**



**Figure 4. A Snapshot of the Animation of the Induction Motor Operation Showing Torque, the Voltage Distribution Along the Circuits of the Inverter**

Figure 3 shows a screen snapshot in which the voltage distribution along the circuits and components of the inverter are displayed with a graph perpendicular to the plane of the inverter. Note that the inverter is represented as a circuit in a plane. The overall display can be rotated, panned and zoomed as the simulation progresses to view the evolution of the voltages from all possible angles. Similar animations can be provided for the electric current

Figure 4 illustrates a snapshot of the induction motor operation. Note that in this particular snapshot, the three-dimensional display of the induction motor is provided. The rotor rotates as the simulation progresses. The torque, stator magnetic flux, rotor magnetic flux and air gap magnetic flux are illustrated on planes perpendicular to the motor axis. The displays of these quantities are continuously updated as the

simulation progresses so as to provide the animation. The entire display can be rotated, panned and zoomed as the simulation progresses to view the evolution of the state of the induction motor from all possible angles. Similar animations can be provided for other physical quantities of the motor.

It is important to note that the system is multitasking allowing multiple animations of the same system. For example one can create an animation of the inverter showing the inverter voltages, another animation of the inverter currents and another animation of the motor position, torque and magnetic fluxes. All these animations can be simultaneously viewed on three different windows.

## Conclusions

The technology for the development of virtual power system laboratories was demonstrated. However, much more work remains to develop a comprehensive library of visualization modules for the plethora of existing power system elements. We have discussed our recent work towards the development of a virtual simulation environment and presented a specific application example of an inverter-driven induction motor. It is clear that virtual laboratories can be quite beneficial from the educational point of view as they can provide insight of the system under study that are impossible in a physical laboratory. The presentation of the paper includes a live demonstration of the inverter-driven induction motor example.

## Acknowledgments

The work reported in this paper has been partially supported by the ONR Grant No. N00014-96-1-0926. This support is gratefully acknowledged.

## References

1. A. P. Sakis Meliopoulos and G. J. Cokkinides, "A Time Domain Model for Flicker Analysis", *Proceedings of the IPST '97*, pp. 365-368, Seattle, WA, June 1997.
2. Eugene V. Solodovnik, George J. Cokkinides and A. P. Sakis Meliopoulos, "Comparison of Implicit and Explicit Integration Techniques on the Non-Ideal Transformer Example", *Proceedings of the Thirtieth Southeastern Symposium on System Theory*, pp. 32-37, West Virginia, March 1998
3. Eugene V. Solodovnik, George J. Cokkinides and A. P. Sakis Meliopoulos, "On Stability of Implicit Numerical Methods in Nonlinear Dynamical Systems Simulation", *Proceedings of the Thirtieth Southeastern Symposium on System Theory*, pp. 27-31, West Virginia, March 1998.
4. Beides, H., Meliopoulos, A. P. and Zhang, F. "Modeling and Analysis of Power System Under Periodic Steady State Controls", *IEEE 35th Midwest Symposium on Circuit and Systems*

5. A. P. Sakis Meliopoulos, *Power System Grounding and Transients*, Marcel Dekker, Inc., 1988.
6. A. P. Sakis Meliopoulos, G. J. Cokkinides and A. G. Bakirtzis, "Load-Frequency Control Service in a Deregulated Environment", *Decision Support Systems*, Vol. 24, No. 3-4, pp. 243-250, January 1999.
7. A. P. Sakis Meliopoulos, Murad Asad and George J. Cokkinides, 'Issues of Reactive Power and Voltage Control Pricing in a Deregulated Environment', *Proceedings of the 32<sup>nd</sup> Annual Hawaii International Conference on System Sciences*, p. 113 (pp. 1-7), Wailea, Maui, Hawaii, January 5-8, 1999.
8. Ben Beker, George J. Cokkinides, Roger Dugal and A. P. Sakis Meliopoulos, 'The Virtual Test Bed for PEBB Based Systems', *Proceedings of the 3rd International Conference on Digital Power System Simulators*, Vasteras, Sweden, May 25-28, 1999.
9. A. P. Sakis Meliopoulos, David Taylor, George J. Cokkinides and Ben Beker 'Small Signal Stability Analysis in PEBB Based Systems', *Proceedings of the 3rd International Conference on Digital Power System Simulators*, Vasteras, Sweden, May 25-28, 1999.
10. A. P. Meliopoulos and George J. Cokkinides 'Small Signal Stability Analysis in PEBB Driven Motion Systems', *Proceedings of the ELECTROMOTION '99 Symposium*, pp. 273-278, Patras, Greece, July 8-9, 1999.

**Biographies**

**A. P. Sakis Meliopoulos** (M '76, SM '83, F '93) was born in Katerini, Greece, in 1949. He received the M.E. and E.E. diploma from the National Technical University of Athens, Greece, in 1972; the M.S.E.E. and Ph.D. degrees from the Georgia Institute of Technology in 1974 and 1976, respectively. In 1971, he worked for Western Electric in Atlanta, Georgia. In 1976, he joined the Faculty of Electrical Engineering, Georgia Institute of Technology, where he is presently a professor. He is active in teaching and research in the general areas of modeling, analysis, and control of power systems. He has made significant contributions to power system grounding, harmonics, and reliability assessment of power systems. He is the author of the books, *Power Systems Grounding and Transients*, Marcel Dekker, June 1988, *Lightning and Overvoltage Protection*, Section 27, Standard Handbook for Electrical Engineers, McGraw Hill, 1993, and the monograph, *Numerical Solution Methods of Algebraic Equations*, EPRI monograph series. Dr. Meliopoulos is a member of the Hellenic Society of Professional Engineering and the Sigma Xi.

**George Cokkinides** (M '85) was born in Athens, Greece, in 1955. He obtained the B.S., M.S., and Ph.D. degrees at the Georgia Institute of Technology in 1978, 1980, and 1985, respectively. From 1983 to 1985, he was a research engineer at the Georgia Tech Research Institute. Since 1985, he has been with the University of South Carolina where he is

presently an Associate Professor of Electrical Engineering. His research interests include power system modeling and simulation, power electronics applications, power system harmonics, and measurement instrumentation. Dr. Cokkinides is a member of the IEEE/PES.

**W. Gao** was born in Jiangxi, China in 1968. He received the Bachelor degree in Engineering from Northwestern Polytechnic University, Xi'an, China, in 1988; the Master degree in industrial automation from Northeastern University, Shenyang, China, in 1991. He is currently working for his Ph.D. degree in the School of Electrical and Computer Engineering in Georgia Institute of Technology.

**Appendix A: Induction Motor Model**

The dynamic equations of the electrical system of an induction machine are derived in this section. The induction machine can be viewed as a set of mutually coupled inductors, which interact among themselves to generate the electromagnetic torque. Straightforward circuit analysis leads to the derivation of an appropriate mathematical model.

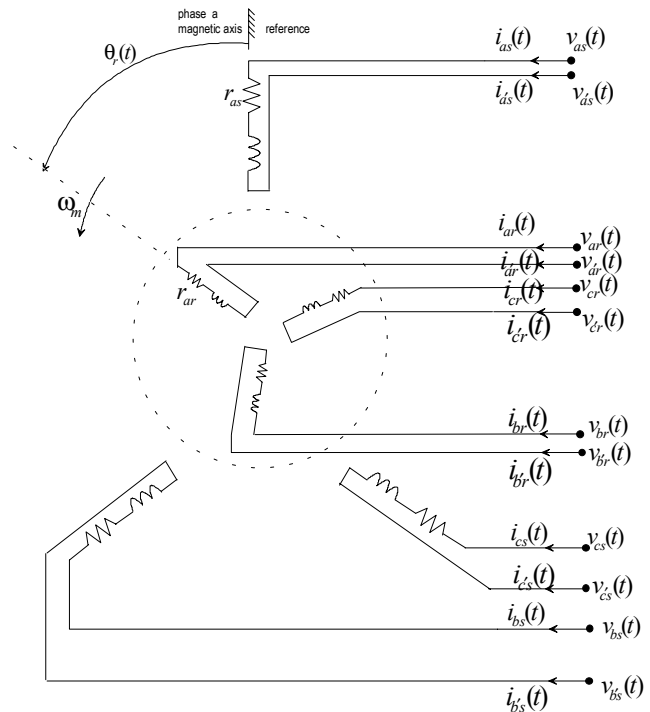


Figure 1. A general induction machine as a set of mutually coupled windings

In the process of derivation, the following assumptions are made: (1) the machine is cylindrical; (2) space mmf and flux waves are sinusoidally distributed (neglecting the teeth and slots effects); (3) the saturation, hysteresis, and eddy currents are neglected. Figure 1 illustrates the stator and rotor windings of an induction machine: three phase stator windings, and three phase rotor windings. The rotor may be

wound rotor or squirrel cage rotor. In either case, the rotor windings can be idealized in the same way as the stator windings. In fact, there is a procedure for representing the squirrel cage by an equivalent set of sinusoidally distributed windings. Note that all inductors are mounted on the same magnetic circuit and thus they are all magnetically coupled. The position of the rotating rotor is denoted with the electrical angle between the stator phase **as** magnetic axis (a stationary reference) and the rotor phase **ar** magnetic axis,  $\theta_r(t)$ . The mechanical rotor position angle is:

$$\theta_m(t) = \frac{2}{p} \theta_r(t) \quad (\text{A.1})$$

where  $p$  is the number of poles of the rotating magnetic field in the air gap.

Application of Kirchhoff's voltage law to the circuit of Figure 1 yields:

$$v_{abcs}(t) - v_{a'b'c's}(t) = R_s i_{abcs}(t) + \frac{d}{dt} \lambda_{abcs}(t) \quad (\text{A.2})$$

$$v_{abcr}(t) - v_{a'b'c'r}(t) = R_r i_{abcr}(t) + \frac{d}{dt} \lambda_{abcr}(t) \quad (\text{A.3})$$

$$i_{a'b'c's}(t) = -i_{abcs}(t) \quad (\text{A.4a})$$

$$i_{a'b'c'r}(t) = -i_{abcr}(t) \quad (\text{A.4b})$$

where

$$v_{abcs}(t) = [v_{as}(t) \quad v_{bs}(t) \quad v_{cs}(t)]^T$$

$$v_{abcr}(t) = [v_{ar}(t) \quad v_{br}(t) \quad v_{cr}(t)]^T$$

$$i_{abcs}(t) = [i_{as}(t) \quad i_{bs}(t) \quad i_{cs}(t)]^T$$

$$i_{abcr}(t) = [i_{ar}(t) \quad i_{br}(t) \quad i_{cr}(t)]^T$$

$$v_{a'b'c's}(t) = [v_{a's}(t) \quad v_{b's}(t) \quad v_{c's}(t)]^T$$

$$v_{a'b'c'r}(t) = [v_{a'r}(t) \quad v_{b'r}(t) \quad v_{c'r}(t)]^T$$

$$i_{a'b'c's}(t) = [i_{a's}(t) \quad i_{b's}(t) \quad i_{c's}(t)]^T$$

$$i_{a'b'c'r}(t) = [i_{a'r}(t) \quad i_{b'r}(t) \quad i_{c'r}(t)]^T$$

$$\lambda_{abcs}(t) = [\lambda_{as}(t) \quad \lambda_{bs}(t) \quad \lambda_{cs}(t)]^T$$

$$\lambda_{abcr}(t) = [\lambda_{ar}(t) \quad \lambda_{br}(t) \quad \lambda_{cr}(t)]^T$$

$$R_s = \text{diag}(r_{as} \quad r_{bs} \quad r_{cs})$$

$$R_r = \text{diag}(r_{ar} \quad r_{br} \quad r_{cr})$$

$$\Gamma = [1 \quad 1 \quad 1]^T$$

$\lambda_{abcs}(t)$  is the vector consisting of the magnetic flux linkages of stator phase **as**, **bs**, and **cs**, respectively.  $\lambda_{abcr}(t)$  is the vector consisting of the magnetic flux linkages of rotor phase **ar**, **br**, and **cr**, respectively. Note that if

$$R_s = \text{diag}(r_s \quad r_s \quad r_s)$$

$$R_r = \text{diag}(r_r \quad r_r \quad r_r)$$

then, we have balanced rotor windings and stator windings.

In Equations (A.2) and (A.3), the magnetic flux linkages are complex functions of the rotor position and the electric currents flowing in the various windings of the machine. The magnetic flux linkages of the phase  $a$ ,  $b$ , and  $c$  are:

$$\begin{bmatrix} \lambda_{abcs}(t) \\ \lambda_{abcr}(t) \end{bmatrix} = \begin{bmatrix} L_{ss} & L_{sr}(t) \\ L_{rs}(t) & L_{rr} \end{bmatrix} \begin{bmatrix} i_{abcs}(t) \\ i_{abcr}(t) \end{bmatrix} \quad (\text{2.5})$$

where

$$L_{ss} = \begin{bmatrix} L_{ls} + L_{ms} & -\frac{1}{2} L_{ms} & -\frac{1}{2} L_{ms} \\ -\frac{1}{2} L_{ms} & L_{ls} + L_{ms} & -\frac{1}{2} L_{ms} \\ -\frac{1}{2} L_{ms} & -\frac{1}{2} L_{ms} & L_{ls} + L_{ms} \end{bmatrix}$$

$$L_{rr} = \begin{bmatrix} L_{lr} + L_{mr} & -\frac{1}{2} L_{mr} & -\frac{1}{2} L_{mr} \\ -\frac{1}{2} L_{mr} & L_{lr} + L_{mr} & -\frac{1}{2} L_{mr} \\ -\frac{1}{2} L_{mr} & -\frac{1}{2} L_{mr} & L_{lr} + L_{mr} \end{bmatrix}$$

$$L_{sr}(t) = L_{sr} \begin{bmatrix} \cos(\theta_r(t)) & \cos(\theta_r(t) + 2\pi/3) & \cos(\theta_r(t) - 2\pi/3) \\ \cos(\theta_r(t) - 2\pi/3) & \cos(\theta_r(t)) & \cos(\theta_r(t) + 2\pi/3) \\ \cos(\theta_r(t) + 2\pi/3) & \cos(\theta_r(t) - 2\pi/3) & \cos(\theta_r(t)) \end{bmatrix}$$

$$L_{rs}(t) = L_{sr}^T(t)$$

The notation in above equations is obvious.  $(L_{ls} + L_{ms})$  is the self-inductance for each of stator windings, and  $L_{ms}$  is the stator magnetizing inductance.  $(L_{lr} + L_{mr})$  is the self-inductance for each of rotor windings, and  $L_{mr}$  is the rotor magnetizing inductance.  $L_{sr}$  is the maximum mutual inductance between a stator phase winding and a rotor phase winding. Notice that the mutual inductances in matrix

$L_{sr}(t)$  are dependent on the position of the rotor, which is time varying. This makes the overall system highly nonlinear and time varying.

The electromagnetic torque is given by the equation:

$$T_{em}(t) = \frac{P_{em}(t)}{\omega_m(t)} = \frac{dw_{fld}(t)}{d\theta_m}$$

It determines the amount of

power converted from electrical power into mechanical power and can be computed by differentiating the field energy function  $w_{fld}(t)$  with respect to the rotor mechanical position  $\theta_m$ . In particular, we have:

$$T_{em}(t) = (i_{abcs}(t))^T \left( \frac{\partial L_{sr}(t)}{\partial \theta_m} \right) i_{abcr}(t)$$

Upon substitution and some manipulations, the rotor equations are expressed in the form:

$$J \frac{d\omega_m(t)}{dt} = (i_{abcs}(t))^T \left( \frac{\partial L_{sr}(t)}{\partial \theta_m} \right) i_{abcr}(t) - T_m(t) \quad (\text{A.6})$$

$$\frac{d\theta_m(t)}{dt} = \omega_m(t) \quad (\text{A.7})$$